Available online at www.sciencedirect.com
ScienceDirect
Journal of Nuclear Materials 375 (2008) 229–242
journal of nuclear materials
www.elsevier.com/locate/jnucmat

Standard molar Gibbs energy of formation of $Pb_5Bi_8O_{17}$ and $PbBi_{12}O_{19}$ and phase diagram of the Pb–Bi–O system

Rajesh Ganesan [a], T. Gnanasekaran [a,*], Raman S. Srinivasa [b]

[a] Liquid Metals and Structural Chemistry Division, Chemistry Group, Indira Gandhi Centre for Atomic Research, Kalpakkam 603 102, India
[b] Department of Metallurgical Engineering and Materials Science, Indian Institute of Technology Bombay, Mumbai 400 076, India

Received 16 March 2007

Abstract

Equilibrium phase fields of the ternary Pb–Bi–O system were established by long-term equilibration in the temperature range 660–840 K. Using these results, the partial phase diagram of the ternary system has been constructed. The standard molar Gibbs energy of formation of the ternary oxides, $\langle Pb_5Bi_8O_{17}\rangle$ and $\langle PbBi_{12}O_{19}\rangle$, was determined by measuring the equilibrium oxygen partial pressures over the relevant phase fields by static manometry in conjunction with a solid oxide electrolyte-based emf cell. Further, the standard molar Gibbs energy of formation of $\langle Pb_3O_4\rangle$ was also measured by the manometric method. The oxide that coexists with the Pb–Bi eutectic alloy (LBE) has been experimentally confirmed as $[\beta\text{-PbO}]_{ss}$. Using the thermochemical data measured, the compositions of Pb–Bi alloys that coexist with $[\beta\text{-PbO}]_{ss}$ and ternary oxides were derived and reported.

1. Introduction

Liquid lead and lead–bismuth eutectic alloys are currently being explored for their service as coolant in nuclear reactors and accelerator driven systems [1]. Owing to its relatively low chemical reactivity, the lead–bismuth eutectic (LBE) alloy is being considered as an alternative to liquid sodium coolant in fast breeder reactors. This eutectic alloy, having a composition of 44.1 at.% Pb and eutectic temperature of 398 K [2], has been extensively used as the coolant in compact nuclear reactors of submarines in Russia [3]. Though pure Pb–Bi coolant is corrosive towards structural steels, a protective oxide layer that prevents this corrosion can be formed over the structural steels by suitable control of oxygen concentration in this alloy [3–5]. The oxygen potential needed for this purpose is maintained in the coolant by reacting it with a mixture of (H_2)–(H_2O) of suitable composition or by passing the coolant through a hot column loaded with a solid solution of lead and bismuth oxide [6]. The extent of dissolution of this oxide and maintenance of the dissolved oxygen level in the LBE are dictated by the thermochemical properties of the oxides involved and the kinetics of their dissolution. Further, the oxide that coexists with LBE under high oxygen potential has not been unequivocally established although it is generally taken as $\langle PbO\rangle$. Martynov and Orlov [6] have analysed the slag over LBE in an operating rig and reported that it contained $\langle PbO\rangle$ (≈48.3 mass%) and $\langle Bi_2O_3\rangle$ (1.7 mass%) apart from $\langle Pb\rangle + \langle Bi\rangle$ (41.8 mass%) along with impurities like $\langle Fe\rangle$ (1.8 mass%), $\langle C\rangle$ (3.3 mass%), $\langle Mg\rangle$ (1.8 mass%), etc.

The pseudo-binary phase diagram of PbO–Bi_2O_3 system has been reported in literature [7] and four ternary compounds are known in this system, viz., $\langle PbBi_{12}O_{19}\rangle$, $\langle Pb_2Bi_6O_{11}\rangle$, $\langle Pb_5Bi_8O_{17}\rangle$ and $\langle Pb_3Bi_2O_6\rangle$ (Fig. 1). Among these compounds, $\langle Pb_2Bi_6O_{11}\rangle$ and $\langle Pb_3Bi_2O_6\rangle$ are stable only over narrow ranges of temperature viz., 848–882 K and 853–876 K, respectively. $\langle PbBi_{12}O_{19}\rangle$ and $\langle Pb_5Bi_8O_{17}\rangle$ are stable from room temperature up to ≈988 K and ≈868 K, respectively. $\langle PbBi_{12}O_{19}\rangle$ exists in cubic form

* Corresponding author. Tel.: +91 44 27480302; fax: +91 44 27480065.
E-mail address: gnani@igcar.gov.in (T. Gnanasekaran).

0022-3115/$ - see front matter © 2008 Elsevier B.V. All rights reserved.
doi:10.1016/j.jnucmat.2008.01.003

Notation

⟨A⟩	solid A	(A)	gas A
{A}	liquid A	$[A]_B$	solution of A in B

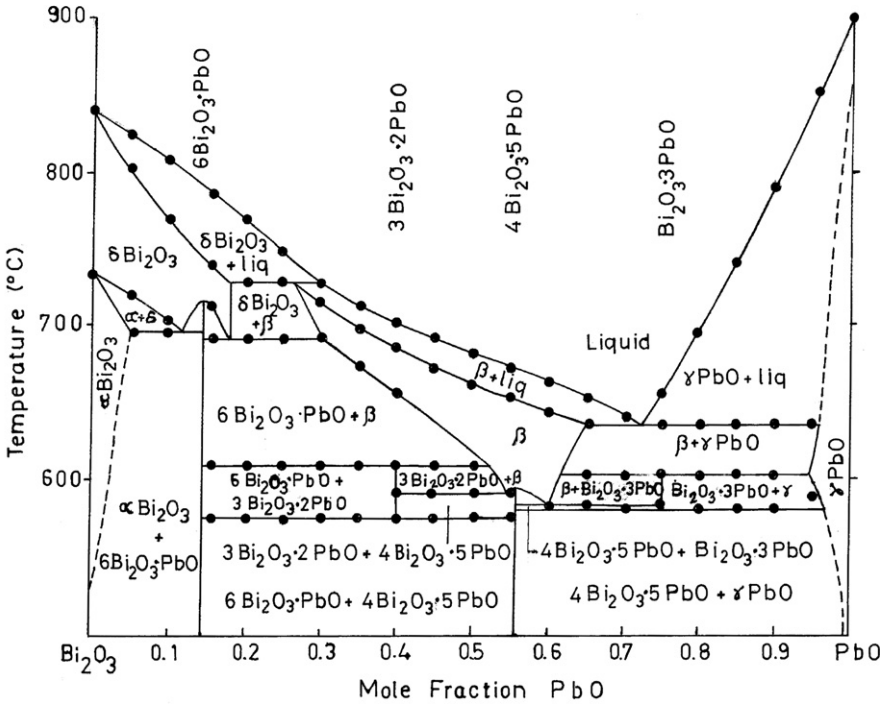

Fig. 1. Phase diagram of the Bi_2O_3–PbO system as given by Biefeld and White [6].

(bcc) [8–10]. Structural aspects of ⟨$Pb_5Bi_8O_{17}$⟩ have been the theme of several studies in the past [7,11–17] and the data reported in literature are compiled in Table 1. It can be seen from Table 1 that ⟨$Pb_5Bi_8O_{17}$⟩ has at least four polymorphs of which ⟨β_1-$Pb_5Bi_8O_{17}$⟩, ⟨β_2-$Pb_5Bi_8O_{17}$⟩ and ⟨ϕ-$Pb_5Bi_8O_{17}$⟩ are low temperature phases. ⟨β-$Pb_5Bi_8O_{17}$⟩ is a high-temperature phase and has a wide range of non-stoichiometry. It exhibits high oxide ion conductivity [11] making it suitable for use as an oxygen selective membrane [18]. ⟨β_1-$Pb_5Bi_8O_{17}$⟩, with monoclinic structure, is formed when quenched in liquid nitrogen from the temperature range of 868–878 K [12]. ⟨β_2-$Pb_5Bi_8O_{17}$⟩, a metastable phase with tetragonal structure is formed at different temperatures [12]. The structure of ⟨ϕ-$Pb_5Bi_8O_{17}$⟩ has been reported to be triclinic [15–17,19,20]. Although the stoichiometry of ⟨ϕ-$Pb_5Bi_8O_{17}$⟩ had been disputed, the recent work of Gemmi et al. [17] confirmed its stoichiometry and its structure to be triclinic. It has been indicated in the literature that the formation of all these phases of ⟨$Pb_5Bi_8O_{17}$⟩ depends on the thermal history of the sample [15,17] and this could be attributed to their comparable thermodynamic stabilities. The structural aspects of ⟨PbO⟩ and ⟨Bi_2O_3⟩ have been discussed elsewhere [21,22].

In the present work, the partial phase diagram of the Pb–Bi–O system was established over the temperature range of 740–840 K. The standard molar Gibbs energy of formation of ⟨$PbBi_{12}O_{19}$⟩ and ⟨$Pb_5Bi_8O_{17}$⟩ was determined by measuring equilibrium oxygen partial pressures over appropriate ternary phase fields by static manometry and by using solid oxide electrolyte-based emf cells. Oxygen partial pressure measurements were also carried out on the well-established ⟨β-PbO⟩–⟨Pb_3O_4⟩ equilibrium. Based on these data, the oxide that coexists with LBE was deduced by computations and also confirmed by experiments.

2. Experimental

2.1. Materials

Lead metal of 5 N purity (M/s. Strem Chemicals, USA) and bismuth metal of 4 N purity (M/s. Nuclear Fuel Complex, India) were used in this work. Ultra high purity (UHP) grade argon and oxygen gases (M/s. Bhoruka Gas Ltd., India) were used. The LBE alloy was prepared by

Table 1
Literature data on structural aspects of $\langle Pb_5Bi_8O_{17}\rangle$

S. no.	Reference	Transformations	[a] Structural details
1.	Biefeld and White [7]	Compound formed at 878 K on cooling	Structure could not be determined by the authors from the powder pattern
2.	Honnart et al. [11]	High-temperature β phase could not be quenched $\beta_2 \overset{723\ K}{\rightarrow} Pb_5Bi_8O_{17} \overset{863\ K}{\rightarrow} \beta$	β: cubic β_2: tetragonal (considered to be metastable)
3.	Bordovskii and Zarkoi [12]	When high-temperature β phase was quenched in liquid nitrogen from the following temperatures monophasic samples was obtained: β_1 (T: 868–878 K) β_2 (T: 843–868 K) Slower cooling resulted in mixture of phases	β_1: monoclinic (given as β by authors) β_2: tetragonal (given as α by authors)
4.	Sammes et al. [13]	$\beta_2 \overset{773\ K}{\rightarrow} Pb_5Bi_8O_{17}$ (mixed state) $\overset{863\ K}{\rightarrow} \beta$	The phases in the temperature range 773–863 K could not be identified
5.	Fee et al. [14]	When $Pb_5Bi_8O_{17}$ was heated at 993 K and rapidly quenched in air, β_2 phase formed Room temperature phase of $Pb_5Bi_8O_{17}$ dependent on the thermal history of the material When β_2 phase was heated below 743 K or above 863 K and cooled to room temperature, phase formed was β_2 only When β_2 phase was heated to intermediate temperatures and quenched in air, phase Φ was formed	Φ-phase reported to be with large unit cell Its structure could not be identified
6.	Watanabe et al. [15]	Stability of β_2 and Φ-phase was found to depend on thermal history of the sample On heating: $\beta_2 \overset{773\ K}{\rightarrow} \Phi$, $\Phi \overset{858\ K}{\rightarrow} \beta$. On cooling: $\beta \overset{833\ K}{\rightarrow} \beta_2$	β: unquenchable cubic phase and stable above 858 K Reported Φ-phase as triclinic (given as β_L by authors) and its composition as $Pb_3Bi_5O_{10.5}$
7.	Zhang et al. [16]	On heating: $\beta_2 \overset{703\ K}{\rightarrow} \Phi$. On cooling: $\beta \overset{863\ K}{\rightarrow} \beta_2$	The phases reported to be present in the intermediate temperatures (703–863 K): Φ, a triclinic compound, tetragonal Pb_3O_4 and monoclinic $Pb_{12}O_{19}$
8.	Gemmi et al. [17]	Three compounds depending on the thermal history of the material On heating: $\beta_2 \overset{673\ K}{\rightarrow} \Phi \overset{858\ K}{\rightarrow} \beta$	Confirmed Φ-phase to be $Pb_5Bi_8O_{17}$ with triclinic structure with no segregation of lead oxides

[a] Although various authors use different notations, a common notation is used here for comparison.

melting a mixture of stoichiometric amounts of ⟨Pb⟩ and ⟨Bi⟩ in an alumina crucible in an argon atmosphere glove box. The alloy was then sealed in a quartz ampoule under vacuum after initially purging the vacuum system with argon gas. The sample in the ampoule was equilibrated at 673 K for 4 days and then quenched in liquid nitrogen. The LBE alloy was characterized by studying its thermal behaviour using DTA technique (M/s. Rheometric Scientific Co., UK). The compound $\langle Pb_3O_4\rangle$, was prepared by oxidising ⟨β-PbO⟩ powder (99.999 mass%, M/s. Aldrich, USA) in a stream of oxygen at 813 K for >12 h. The ternary compounds $\langle PbBi_{12}O_{19}\rangle$ and $\langle Pb_5Bi_8O_{17}\rangle$ were prepared by solid-state reaction between ⟨β-PbO⟩ and $\langle Bi_2O_3\rangle$ (99.99 mass%, M/s. Nuclear Fuel Complex, India) powders taken in stoichiometric mole ratios. The oxide powders were mixed thoroughly, ground using a mortar and pestle and compacted into discs. The discs were taken in alumina crucibles, which in turn were placed inside one-end closed quartz tubes. These tubes were repeatedly evacuated after filling 2–3 times with argon gas and sealed under vacuum. $\langle PbBi_{12}O_{19}\rangle$ was prepared by heating the oxide mixture at 908 K for 200 h, while $\langle Pb_5Bi_8O_{17}\rangle$ was prepared by heating at 823 K for 200 h with one intermediate grinding, mixing, pelletising and vacuum sealing. The products were cooled slowly (≈5 K/min) after the heat treatment. The compounds prepared were characterised by X-ray diffraction using a Siemens D500 X-ray powder diffractometer with Cu Kα radiation and graphite monochromator. The XRD patterns of $\langle Pb_3O_4\rangle$, $\langle PbBi_{12}O_{19}\rangle$ and $\langle Pb_5Bi_8O_{17}\rangle$ matched with the patterns reported in JCPDS files of these compounds, viz., 41–1493, 24–1184 and 52–1497, respectively [23].

2.2. Phase equilibrium studies

Mixtures of various phases (Table 2) were made by mixing and grinding the component phases in an agate mortar. The overall composition of the phase mixture based on the amount of starting phases is also given in Table 2. The overall compositions were chosen such that the ternary phase diagram could be established without any ambiguity. When metallic lead or bismuth was one of the components,

Table 2
Results of phase equilibrium studies on the Pb–Bi–O system

S. no.	Starting phases before equilibration	Overall composition	Temperature of equilibration (K)[a]	Phases identified after equilibration
Compositions above the pseudo-binary $PbO–Bi_2O_3$ line				
1	⟨β-PbO⟩, ⟨Pb_3O_4⟩	$Pb_{0.43}O_{0.57}$	823	⟨β-PbO⟩, ⟨Pb_3O_4⟩
2.a	⟨β-PbO⟩, ⟨Pb_3O_4⟩, ⟨$PbBi_{12}O_{19}$⟩	$Pb_{0.13}Bi_{0.29}O_{0.58}$	823	⟨Pb_3O_4⟩, ⟨ϕ-$Pb_5Bi_8O_{17}$⟩, ⟨$PbBi_{12}O_{19}$⟩
2.b	⟨Pb_3O_4⟩, ⟨ϕ-$Pb_5Bi_8O_{17}$⟩, ⟨$PbBi_{12}O_{19}$⟩	$Pb_{0.13}Bi_{0.29}O_{0.58}$	740, 823, 840	⟨Pb_3O_4⟩, ⟨ϕ-$Pb_5Bi_8O_{17}$⟩, ⟨$PbBi_{12}O_{19}$⟩
3	Pb_3O_4⟩, ⟨ϕ-$Pb_5Bi_8O_{17}$⟩, ⟨$PbBi_{12}O_{19}$⟩	$Pb_{0.23}Bi_{0.19}O_{0.58}$	823	⟨Pb_3O_4⟩, ⟨ϕ-$Pb_5Bi_8O_{17}$⟩, ⟨$PbBi_{12}O_{19}$⟩
4.a	⟨β-PbO⟩, ⟨Pb_3O_4⟩, ⟨Bi_2O_3⟩	$Pb_{0.31}Bi_{0.14}O_{0.55}$	740, 840	⟨β-PbO⟩, ⟨Pb_3O_4⟩, ⟨β_1⟩ and ⟨β_2-$Pb_5Bi_8O_{17}$⟩
4.b	⟨β-PbO⟩, ⟨Pb_3O_4⟩, ⟨ϕ-$Pb_5Bi_8O_{17}$⟩	$Pb_{0.31}Bi_{0.14}O_{0.55}$	740, 840	⟨β-PbO⟩, ⟨Pb_3O_4⟩, ⟨β_1⟩ and ⟨β_2-$Pb_5Bi_8O_{17}$⟩
Compositions below the pseudo-binary $PbO–Bi_2O_3$ line				
5.a	⟨Pb⟩, ⟨β-PbO⟩, ⟨Bi_2O_3⟩	$Pb_{0.35}Bi_{0.15}O_{0.50}$	660, 823	⟨Bi⟩, [β-PbO]$_{ss}$, ⟨ϕ-$Pb_5Bi_8O_{17}$⟩
5.b	⟨Bi⟩, ⟨β-PbO⟩, ⟨Bi_2O_3⟩	$Pb_{0.35}Bi_{0.15}O_{0.50}$	823	⟨Bi⟩, [β-PbO]$_{ss}$, ⟨ϕ-$Pb_5Bi_8O_{17}$⟩
6.a	⟨Pb⟩, ⟨β-PbO⟩, ⟨Bi_2O_3⟩	$Pb_{0.13}Bi_{0.32}O_{0.55}$	823	⟨Bi⟩, ⟨ϕ-$Pb_5Bi_8O_{17}$⟩, ⟨$PbBi_{12}O_{19}$⟩
6.b	⟨Bi⟩, ⟨β-PbO⟩, ⟨Bi_2O_3⟩	$Pb_{0.13}Bi_{0.32}O_{0.55}$	823	⟨Bi⟩, ⟨ϕ-$Pb_5Bi_8O_{17}$⟩, ⟨$PbBi_{12}O_{19}$⟩
7.a	⟨Pb⟩, ⟨β-PbO⟩, ⟨Bi_2O_3⟩	$Pb_{0.22}Bi_{0.28}O_{0.50}$	823	⟨Bi⟩, [β-PbO]$_{ss}$, ⟨ϕ-$Pb_5Bi_8O_{17}$⟩
7.b	⟨Bi⟩, ⟨β-PbO⟩, ⟨Bi_2O_3⟩	$Pb_{0.22}Bi_{0.28}O_{0.50}$	823	⟨Bi⟩, [β-PbO]$_{ss}$, ⟨ϕ-$Pb_5Bi_8O_{17}$⟩
8.a	⟨Pb⟩, ⟨Bi⟩, ⟨Bi_2O_3⟩	$Pb_{0.10}Bi_{0.40}O_{0.50}$	823	⟨Bi⟩, ⟨ϕ-$Pb_5Bi_8O_{17}$⟩, ⟨$PbBi_{12}O_{19}$⟩
8.b	⟨Bi⟩, ⟨β-PbO⟩, ⟨Bi_2O_3⟩	$Pb_{0.10}Bi_{0.40}O_{0.50}$	823	⟨Bi⟩, ⟨ϕ-$Pb_5Bi_8O_{17}$⟩, ⟨$PbBi_{12}O_{19}$⟩
9.a	⟨Pb⟩, ⟨Bi⟩, ⟨Bi_2O_3⟩	$Pb_{0.20}Bi_{0.45}O_{0.35}$	823, 840	⟨Bi⟩, [β-PbO]$_{ss}$, ⟨ϕ-$Pb_5Bi_8O_{17}$⟩
9.b	⟨Pb⟩, ⟨β-PbO⟩, ⟨Bi_2O_3⟩	$Pb_{0.20}Bi_{0.45}O_{0.35}$	823	⟨Bi⟩, [β-PbO]$_{ss}$, ⟨ϕ-$Pb_5Bi_8O_{17}$⟩
10	⟨Pb⟩, ⟨β-PbO⟩, ⟨Bi_2O_3⟩	$Pb_{0.54}Bi_{0.35}O_{0.11}$	823	⟨Bi⟩, ⟨Pb_7Bi_3⟩, [β-PbO]$_{ss}$
11	⟨Bi⟩, ⟨β-PbO⟩, ⟨Bi_2O_3⟩	$Pb_{0.69}Bi_{0.21}O_{0.10}$	823	⟨Pb_7Bi_3⟩, ⟨Pb⟩, [β-PbO]$_{ss}$

[a] Duration of equilibration in all cases was ≈200 h.

fine granules of the same were used. The resulting powders were compacted into pellets, taken in an alumina crucible and encapsulated in a quartz ampoule as described earlier. All the equilibrations were carried out at different isothermal temperatures for a total period of ≈200 h, with one intermediate grinding and recompaction. After equilibration, the samples were cooled by quenching the sealed ampoules in liquid nitrogen. The samples were then analysed by X-ray diffraction to deduce the coexisting phases. Equilibrium oxygen pressures in phase mixtures with ⟨Pb_3O_4⟩ as one of the coexisting phase are expected to be high. Hence, due care was taken regarding the size of the samples whose overall composition lies above the pseudo-binary line of $PbO–Bi_2O_3$, so that equilibrium oxygen pressures could be established in the sealed quartz ampoules.

2.3. Manometric measurements

Ultra high vacuum (UHV) assemblies were used to measure the equilibrium oxygen pressures as shown in Fig. 2. All metal flanges with copper gaskets were used for the various joints in the assemblies and metal bellows valves were used. A one end closed quartz tube of 30 mm diameter to house the samples was attached to the vacuum assembly through a flanged joint. The quartz tube was attached to the flange using Torr seal® and the flange had provision to introduce a thermocouple very near the sample placed at the bottom. The quartz tube was placed in the constant temperature zone of a nichrome wire-wound furnace. Additionally, a 100 mm long hollow cylindrical stainless steel block was placed in the constant temperature zone of the furnace to further enhance the temperature uniformity. The temperature of the furnace was measured using a K-type thermocouple and could be controlled with in ±0.2 K using a PID temperature controller. A capacitance manometer (M/s. MKS, USA, model: Baratron), which can measure the pressures in the range of 0–5000 Torr (0–667 kPa) with a resolution of 0.5 Torr (66.7 Pa), was attached to the vacuum line through a flange and was used for measuring the equilibrium oxygen pressures over the phase mixtures. Before the equilibrium oxygen pressure measurements, the whole assembly without any samples in it, was first evacuated to 0.1 Pa, degassed at ≈373 K and tested for its leak tightness for 4 days. The increase in total pressure was ≈0.2 kPa in 4 days. During the equilibrium oxygen pressure measurements, the pressure difference between the interior of the experimental assembly and the ambient air ranged between 10 and 100 kPa and the maximum time of equilibration was 2 days only. Hence, reliable pressure measurements could be made with this experimental assembly. Equilibrium oxygen pressures over the following phase equilibrium mixtures were measured in this work: (1) ⟨Pb_3O_4⟩–⟨β-PbO⟩, (2) ⟨Pb_3O_4⟩–[β-PbO]$_{ss}$–⟨$Pb_5Bi_8O_{17}$⟩ and (3) ⟨Pb_3O_4⟩–⟨$PbBi_{12}O_{19}$⟩–⟨$Pb_5Bi_8O_{17}$⟩. For the measurement of equilibrium oxygen pressures over the ⟨Pb_3O_4⟩–⟨β-PbO⟩ system, the vacuum assembly with an overall volume of 220 cm^3 (Fig. 2(a)) was used and the assembly shown in Fig. 2(b) (overall volume = 95 cm^3) was used for experiments with the other two systems studied. Attempts to measure the equilibrium oxygen pressures

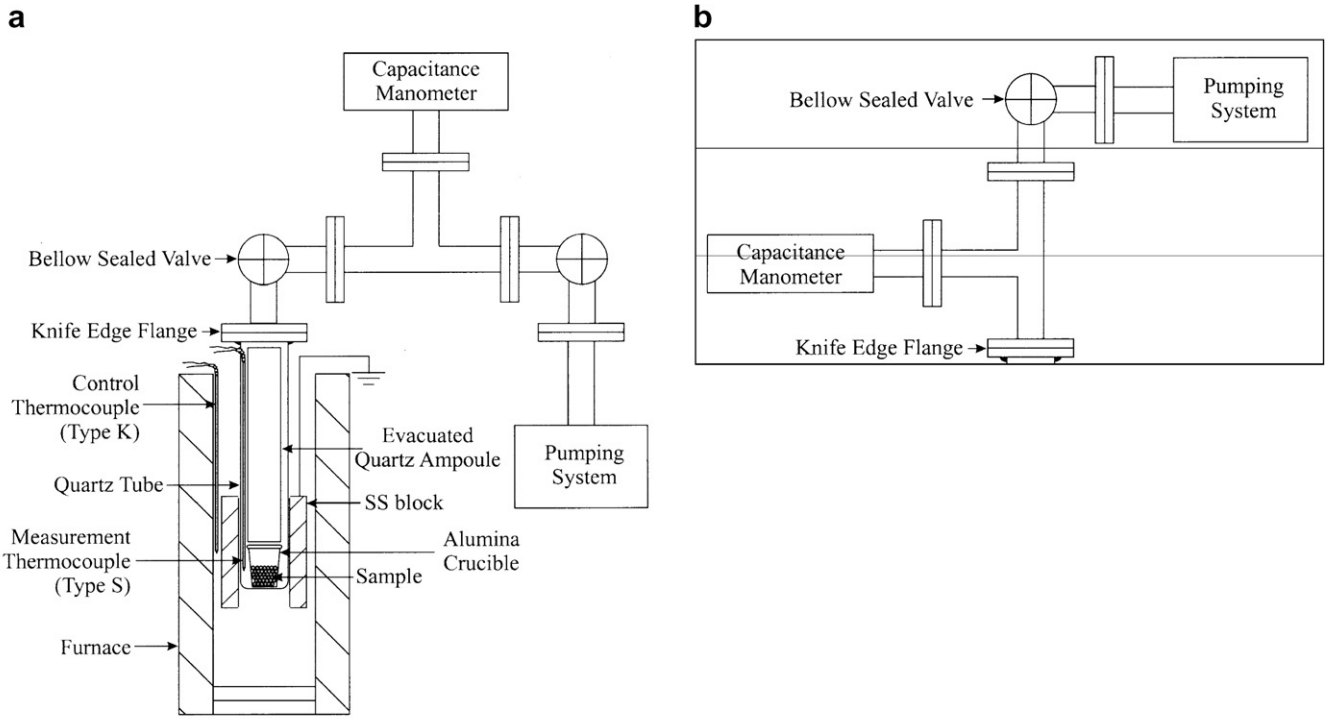

Fig. 2. Scheme of the vacuum assemblies used for measuring equilibrium oxygen pressures in different phase fields: (a) system used for studies on $\langle Pb_3O_4\rangle$–$\langle$β-PbO$\rangle$ system (free volume = 220 cm^3) and (b) system used for studies on $\langle Pb_3O_4\rangle$–$[$β-PbO$]_{ss}$–$\langle Pb_5Bi_8O_{17}\rangle$ and $\langle Pb_3O_4\rangle$–$\langle PbBi_{12}O_{19}\rangle$–$\langle Pb_5Bi_8O_{17}\rangle$ systems (free volume = 95 cm^3).

over $\langle Pb_3O_4\rangle$–$\langle PbBi_{12}O_{19}\rangle$–$\langle Bi_2O_3\rangle$ did not yield reproducible results.

The constituents of the phase equilibrium mixtures used for the oxygen pressure measurements were thoroughly ground together and compacted into pellets of 16 mm diameter and ≈10 mm thick under a pressure of 25 MPa so as to form porous pellets. The resulting porous pellets were placed in a recrystallised alumina crucible, which was in turn kept inside the quartz vessel. The experimental assembly was first evacuated at room temperature and this was continued with the sample heated to 473 K for 24 h to remove any adsorbed gaseous impurities. After isolating the pumping modules, the sample temperature was increased to the experimental temperature and allowed to equilibrate. The pressure and temperature data were recorded every 300 s and were acquired through a multichannel data acquisition system (M/s. Agilent Technologies, USA, model: 34970A data acquisition/switch unit) through an IBM PC using RS232 interface. The time required to attain equilibrium depended on the system studied and the temperature of measurement. The time required for attaining equilibrium pressures with the $\langle Pb_3O_4\rangle$–$\langle$β-PbO$\rangle$ system was lower (≈10 h at ≈760 K and ≈5 h at ≈850 K) than that required for the $\langle Pb_3O_4\rangle$–$[$β-PbO$]_{ss}$–$\langle Pb_5Bi_8O_{17}\rangle$ system (≈12 h at ≈740 K and ≈ 6 h at ≈850 K), which in turn was lower than that encountered with the $\langle Pb_3O_4\rangle$–$\langle Pb_5Bi_8O_{17}\rangle$–$\langle PbBi_{12}O_{19}\rangle$ system (≈18 h at ≈780 K and ≈10 h at ≈850 K). The test of equilibrium was carried out by partially evacuating the assembly and allowing the system to regain its equilibrium pressure. It was also tested by increasing the partial pressure of oxygen in the assembly by addition of small amounts of high purity oxygen to it and allowing the system to retrace to its equilibrium pressure. After achieving equilibrium, the stability of pressures was monitored at least for 5 h before making the measurements. The chemical compatibility of recrystallised alumina with the phase mixtures was found to be excellent in the entire temperature ranges of measurement. The capacitance manometer was calibrated with respect to atmospheric pressure and vacuum, before and after each experiment and the calibration constants were found to remain unchanged during these measurements. The samples were analysed by XRD to identify the coexisting phases before and after the experiments.

2.4. Emf studies

The following two galvanic cells were studied in this work:

$$(-)\text{Kanthal},\langle \text{Ir}\rangle,\{\text{Bi}\},\langle Bi_2O_3\rangle \mid \text{CSZ} \mid (O_2, 101.325\text{kPa}),\text{Pt}(+) \quad \text{(Cell-I)}$$

$$(-)\text{Kanthal},\langle \text{Ir}\rangle,\{\text{Bi}\}_{\text{Pb–Bi}},[\beta-\text{PbO}]_{ss},\langle Pb_5Bi_8\ O_{17}\rangle \mid \text{CSZ} \mid (O_2, 101.325\text{kPa}),\text{Pt}(+) \quad \text{(Cell-II)}$$

One end closed 11 m/o calcia stabilised zirconia (CSZ) solid electrolyte tubes with flat bottom (13 mm OD, 9 mm ID and 250 mm long) supplied by M/s. Nikkato Corporation, Japan were used for constructing the galvanic cells. For both Cell-I, Cell-II, the same electrolyte tube was used. The reference electrode for the cell was prepared by applying platinum paste (M/s. Eletecks Corporation, India) over the inner bottom surface of the electrolyte tube and heating it at 1073 K for 5 h in air. This resulted in a uniform and porous platinum film over the electrolyte surface. A Pt wire co-fired with the platinum paste served as the electrical lead. This arrangement of having the reference electrode at the inner side of the electrolyte tube enabled easier replacement of sample electrodes after thorough cleaning of the outer surface of the electrolyte. The sample electrode for Cell-I was made from a mixture of $\{Bi\}$–$\langle Bi_2O_3\rangle$ in the weight ratio of 10:1 taken inside a recrystallised alumina crucible. For Cell-II, a mixture of $\langle\beta\text{-PbO}\rangle$, $\langle Bi\rangle$ and $\langle Pb_5Bi_8O_{17}\rangle$ with a weight ratio of 1:5:1 was used. The constituents of the mixture were first taken inside another recrystallised alumina crucible, sealed in a quartz ampoule and equilibrated at 843 K for 4 days. The electrolyte tube was later dipped into the sample mixture by heating the latter to ≈473 K in an argon atmosphere glove box. Since iridium is compatible with both Pb and Bi, a short iridium wire (0.5 mm diameter and 30 mm long, M/s. Goodfellow Cambridge Limited, England) spot-welded to a Kanthal wire was used as the electrical lead for the sample electrode. The construction of the emf cell and other experimental details are described elsewhere [21,22]. The cell was housed in a quartz tube using an O-ring seal. This arrangement had provisions for measuring the cell temperature and for flowing high purity argon and oxygen gases through the sample and reference compartments, respectively. The cell assembly was placed in the constant temperature zone of the furnace. Additionally a 100 mm long, hollow cylindrical stainless steel block was placed in the constant temperature zone of the furnace to further enhance the uniformity of the temperature in the zone and the cell temperature could be controlled within ±0.2 K using a PID temperature controller. The stainless steel block was grounded to avoid any a.c. pickup in the emf signal. The cell temperature was measured using a K-type thermocouple and this thermocouple was calibrated prior to actual experiments against a standard calibrated thermocouple supplied by National Physical Laboratory, India. The cell emf was measured using a high impedance electrometer (input impedance $>10^{14}\,\Omega$, Keithley model-617) and the temperature was measured using a multimeter (Hewlett–Packard model-34401 A). The data were acquired through an IBM PC using a GPIB interface.

The thermo emf due to the dissimilar electrical leads viz., Kanthal-platinum were measured as a function of temperature and used for correcting the cell emf. As the junction between Kanthal and Ir was present in the constant temperature zone of the furnace along with the sensor head, the thermo emf due to Kanthal-Ir need not be considered. Measurements were carried out for several heating, cooling and random cycles. Generally the emf values became steady within 10 min after attaining a stable cell temperature. The readings were taken when the cell emf values were stable within $\pm 5 \times 10^{-5}$ V and the stability of the output was monitored at least for 1 h when the temperatures were above 750 K and for at least 3–4 h when the temperatures were below 750 K before making the measurements. The reproducibility of the cell emf was checked by micro polarisation and thermal cycling. After completion of emf measurements, the samples were analysed by XRD to identify the coexisting phases.

2.5. Equilibration experiments in LBE at 823 K

With a view to ascertain the oxide that coexists with LBE, additional equilibration studies were carried out in liquid LBE saturated with oxygen. LBE was taken in alumina crucible and adequate quantity of oxygen was added to it as $\langle\beta\text{-PbO}\rangle$ so that oxygen content in the mixture was three times the solubility of oxygen in LBE at 823 K [24]. Thick films of the compounds $\langle PbBi_{12}O_{19}\rangle$ and $\langle Pb_5Bi_8O_{17}\rangle$ were coated on alumina substrates (5 mm width, 25 mm length, 1 mm thick) possessing a rough surface finish using water as the dispersant medium. The films were dried, annealed at 773 K for 2 h in argon atmosphere to ensure their adherence to the substrates and characterized by XRD. The LBE alloy was heated to ≈473 K inside an argon atmosphere glove box and the coated substrates were inserted into it. The substrates were held in the immersed condition by tying them to the alumina crucible using nichrome wires to avoid their floating and the alloy was then cooled slowly. The alumina crucible was later sealed in an evacuated quartz ampoule and was equilibrated for 2 days at 823 K. The amount of LBE alloy taken for the equilibration was ≈6.3 g. The masses of oxide films were ≈50 mg each and $\langle\beta\text{-PbO}\rangle$ added to LBE was about 12 mg. The quantities of the compounds were low compared to that of LBE taken (≈6.3 g) so that even if they completely dissolved in the alloy, the composition of LBE would not be significantly altered. The substrates were retrieved after equilibration and the XRD pattern of the adhering phases were again recorded.

3. Results and discussion

3.1. Phase equilibrium studies

The results of the phase equilibrium studies are summarised in Table 2. The table lists the compounds/elements taken, together with the composition expressed in mole fractions. As observed in our earlier study, only the high-temperature form of lead oxide, viz., $\langle\beta\text{-PbO}\rangle$ was present throughout our study due to sluggish kinetics of α to β transformation [21]. The initial compositions of the mixtures are shown in Fig. 3 by filled circles. Results of the phase analyses after the equilibration in sealed capsules are also given in

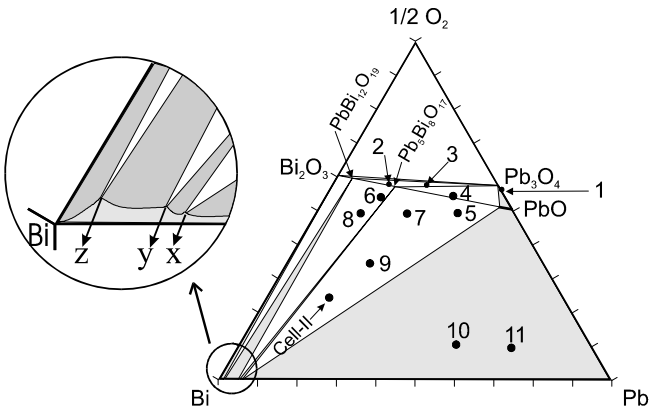

Fig. 3. Isothermal section of the partial phase diagram of the Pb–Bi–O system at 823 K. Filled circles represent nominal compositions of mixtures chosen for equilibration studies. The existence of phase fields (i) $\{Bi\}_{Pb\text{-}Bi}$–$[\beta\text{-PbO}]_{ss}$–$\langle Pb_5Bi_8O_{17}\rangle$, T: 668–837 K, (ii) $\langle Pb_3O_4\rangle$–$[\beta\text{-PbO}]_{ss}$–$\langle Pb_5Bi_8O_{17}\rangle$, T: 745–853 K and (iii) $\langle Pb_3O_4\rangle$–$\langle Pb_5Bi_8O_{17}\rangle$–$\langle PbBi_{12}O_{19}\rangle$, T: 784–848 K have been established. (a) The inset indicates the schematics of the bismuth rich region. (b) The composition at the Bi rich alloy is shown schematically for clarity. (c) Calculated compositions of alloys x, y and z are given in Table 8. (d) The composition of $[\beta\text{-PbO}]_{ss}$ of $[\beta\text{-PbO}]_{ss}$–$[Pb\text{–}Bi]_{alloy\ x}$–$\langle Pb_5Bi_8O_{17}\rangle$ phase field is also shown schematically.

Table 2. The overall compositions of the samples used for equilibration and the analysis of the phases obtained after quenching them to ambient temperature confirmed the following phase fields: (i) $[\beta\text{-PbO}]_{ss}$–$\langle Pb_3O_4\rangle$–$\langle Pb_5Bi_8O_{17}\rangle$, (ii) $\langle Pb_3O_4\rangle$–$\langle Pb_5Bi_8O_{17}\rangle$–$\langle PbBi_{12}O_{19}\rangle$, (iii) $\{Bi\}_{Pb\text{-}Bi}$–$\langle Pb_5Bi_8O_{17}\rangle$–$\langle PbBi_{12}O_{19}\rangle$, (iv) $\{Bi\}_{Pb\text{-}Bi}$–$[\beta\text{-PbO}]_{ss}$–$\langle Pb_5Bi_8O_{17}\rangle$ and (v) $\{Bi\}_{Pb\text{-}Bi}$–$\{Pb\}$–$[\beta\text{-PbO}]_{ss}$. It is to be pointed out that in the case of samples with overall compositions 10 and 11, the phases identified after equilibration and cooling them to ambient temperature were $\langle Bi\rangle$–$\langle Pb_7Bi_3\rangle$–$[\beta\text{-PbO}]_{ss}$ and $\langle Pb_7Bi_3\rangle$–$\langle Pb\rangle$–$[\beta\text{-PbO}]_{ss}$, respectively. As seen from phase diagram of the Pb–Bi system [2], $\langle Pb_7Bi_3\rangle$ would be one of the coexisting phases below the eutectic temperature of 398.5 K, when the Pb content in the Pb–Bi alloys is below 60 at.%. This is in accordance from the observations made with the samples 10 and 11.

It is to be mentioned that the existence of the phase field $\langle Pb_3O_4\rangle$–$\langle Pb_5Bi_8O_{17}\rangle$–$\langle PbBi_{12}O_{19}\rangle$, could be inferred from the thermal analysis of the PbO–Bi_2O_3 system carried out by Braileanu et al. [25]. In the phase fields (ii)–(iv), $\langle Pb_5Bi_8O_{17}\rangle$ was found to be present in a triclinic phase (ϕ) while in the phase field (i) $\langle Pb_5Bi_8O_{17}\rangle$ was found to be a mixture of monoclinic (β_1) and tetragonal (β_2) phases. This result indicates that the relative thermodynamic stabilities of the low temperature phases, viz., β_1, β_2 and ϕ are comparable. A similar conclusion has been derived by Gemmi et al. [17]. Hence, the thermochemical data reported in this work for the compound $\langle Pb_5Bi_8O_{17}\rangle$ is not attributable to any particular phase. The presence of $[\beta\text{-PbO}]_{ss}$ was identified from the shift in the peak positions (≈0.05–0.10°) in the XRD pattern to higher values compared to that of pure β-PbO. The inclusion of Bi^{+3} ion in place of Pb^{+2} decreases the lattice parameter since the size of the Bi^{+3} ion is smaller than the size of the Pb^{+2} ion. This leads to a decrease in the d-spacing. However, the observed shift in the peak positions is very small indicating the amount of Bi_2O_3 present in the $[\beta\text{-PbO}]_{ss}$ is low. Using these data, the phase diagram of the Pb–Bi system [2] and the pseudo-binary phase diagram of PbO–Bi_2O_3, the partial phase diagram of the Pb–Bi–O system was constructed and is shown in Fig. 3. The equilibrium oxygen partial pressures over the following three-phase fields were measured by the manometric technique: (1) $[\beta\text{-PbO}]_{ss}$–$\langle Pb_3O_4\rangle$–$\langle Pb_5Bi_8O_{17}\rangle$ and (2) $\langle Pb_3O_4\rangle$–$\langle Pb_5Bi_8O_{17}\rangle$–$\langle PbBi_{12}O_{19}\rangle$. In addition, equilibrium oxygen pressures over $\langle\beta\text{-PbO}\rangle$–$\langle Pb_3O_4\rangle$ were also measured. The equilibrium oxygen potentials of the three-phase field, $\{Bi\}_{Pb\text{-}Bi}$–$[\beta\text{-PbO}]_{ss}$–$\langle Pb_5Bi_8O_{17}\rangle$ were measured by oxide electrolyte-based emf cells.

3.2. Standard molar Gibbs energy of formation of $\langle Pb_3O_4\rangle$

The measured oxygen partial pressures of the following equilibrium at different experimental temperatures are given in Table 3.

$$3\langle\beta\text{-PbO}\rangle + 1/2(O_2) \Longleftrightarrow \langle Pb_3O_4\rangle. \quad (1)$$

The dependence of the oxygen partial pressure on temperature was obtained by least-squares fitting of the data and is given by the following expression:

$$\log(p(O_2)/\text{kPa}) \pm 0.02 = 12.07\text{–}8697/T \quad (761\text{–}853\ \text{K}). \quad (2)$$

The error given is the standard deviation from the straight line.

The standard Gibbs energy change of reaction (1), $\Delta_rG^\circ(T)$ is given as

$$\Delta_rG^\circ(T) = \Delta_fG^\circ{}_m\langle Pb_3O_4\rangle - 3\Delta_fG^\circ{}_m\langle\beta\text{-PbO}\rangle = (1/2)RT\ln p(O_2). \quad (3)$$

The values of $\Delta_rG^\circ(T)$ can be calculated from oxygen pressure data given by Eq. (2) as

Table 3
Measured equilibrium oxygen pressures over $\langle Pb_3O_4\rangle$–$\langle\beta\text{-PbO}\rangle$ at different temperatures

T(K)	$p(O_2)$ (kPa)	t (h)[a]
760.5	4.16	20
784.3	10.25	19
791.1	11.68	18
800.3	16.47	17
811.5	21.64	16
812.0	22.12	16
816.8	27.14	15
824.9	32.49	14
829.3	37.10	13
834.9	46.69	12
835.4	41.85	12
845.0	59.76	11
853.4	79.53	10

[a] Approximate time taken for equilibrium measurement.

$$\Delta_r G^\circ(\mathrm{T}) \pm 0.16\ \mathrm{kJ} = -83.27 + 0.0963\ T(\mathrm{K}) \quad (761\text{–}853\ \mathrm{K}). \tag{4}$$

The standard molar Gibbs energy of formation of $\langle Pb_3O_4\rangle$ was computed from Eq. (3) using the data given by Eq. (4) and $\Delta_f G^\circ{}_m\langle\beta\text{-PbO}\rangle$ values from our earlier work [21] and is given by

$$\Delta_f G^\circ{}_m\langle Pb_3O_4\rangle \pm 0.34\ \mathrm{kJ} = -740.21 + 0.3952\ T(\mathrm{K}) \quad (761\text{–}853\ \mathrm{K}). \tag{5}$$

Data on $\Delta_f G^\circ{}_m\langle Pb_3O_4\rangle$ have been reported in the literature based on similar measurements of the oxygen partial pressures by manometry [26–30] and also by the emf method [31], and these are listed along with the present data in Table 4. The experimentally measured oxygen pressures from all these references are compared in Fig. 4. This figure also shows the oxygen pressures deduced from the emf data reported in Ref. [31]. As seen from the figure, the present data are in close agreement with the data reported by Reinders and Hamburger [27], Otto [28] and Kharif et al. [30]. The figure also shows that the oxygen pressures reported by Le Chatelier [26] and by Abadir et al. [29] and those calculated from the emf data reported by Mallika and Sreedharan [31] are in disagreement with the present data and are distinctly lower from the rest of the data. It is to be pointed out that the total number of data points reported by Le Chatelier [26] and Abadir et al. [29] were only 4 in both the cases. Abadir et al. [29] had determined the decomposition temperature of $\langle Pb_3O_4\rangle$ at a fixed oxygen pressure by thermogravimetric analysis. The decomposition temperature of $\langle Pb_3O_4\rangle$ to yield $\langle\beta\text{-PbO}\rangle$ and oxygen ($p(O_2) = 101.325$ kPa) calculated from the data reported by Mallika and Sreedharan [31] is 912 K compared to 901 K given by Knacke et al. [32] and 868 K given by Massalski [2]. The data from the present study are in good agreement with the majority of data generated by manometry. This also indicates that the present experimental assembly can reliably be used for measurement of the equilibrium oxygen pressures.

3.3. Standard molar Gibbs energy of formation of $\langle Pb_5Bi_8O_{17}\rangle$

To determine the standard molar Gibbs energy of formation of $\langle Pb_5Bi_8O_{17}\rangle$, oxygen potentials were measured in the phase field $\{Bi\}_{Pb\text{-}Bi}$–$[\beta\text{-PbO}]_{ss}$–$\langle Pb_5Bi_8O_{17}\rangle$ as a function of temperature by using the emf of Cell-II mentioned earlier. The performance of the electrochemical cell was first tested with measurements on the following equilibrium (Cell-I):

$$2\{Bi\} + 3/2(O_2) \Longleftrightarrow \langle Bi_2O_3\rangle. \tag{6}$$

The temperature dependence of measured emf values are given by the expression (7). The standard molar Gibbs energy data of $\langle Bi_2O_3\rangle$, deduced from emf data, are given by expression (8).

$$E_I \pm 0.0005\ \mathrm{V} = 1.0034\text{–}5.018 \times 10^{-4}\ T(\mathrm{K}) \quad (719\text{–}965\ \mathrm{K}), \tag{7}$$

$$\Delta_f G^\circ{}_m\langle\alpha\text{-}Bi_2O_3\rangle \pm 0.3\ \mathrm{kJ} = -580.9 + 0.2905\ T(\mathrm{K}) \quad (719\text{–}965\ \mathrm{K}). \tag{8}$$

These results are in excellent agreement with the data reported in our earlier work [22]. As mentioned earlier, the same electrolyte tube was used in Cell-II by changing the sample electrode.

Emf values obtained from Cell-II are given in Table 5. The variation of cell emf with temperature is given by the following least-squares fitted expression:

$$E_{II} \pm 0.0006\ \mathrm{V} = 1.0236\text{–}5.248 \times 10^{-4}\ T(\mathrm{K}) \quad (668\text{–}837\ \mathrm{K}). \tag{9}$$

Table 4
Comparison of the $\Delta_f G^\circ{}_m\langle Pb_3O_4\rangle$ values reported in the literature

S. no.	$\Delta_f G^\circ{}_m = -A + BT$ (kJ mol^{-1})	Temperature range (K)	$\Delta_f G^\circ{}_m\langle Pb_3O_4\rangle$ (kJ mol^{-1})			No. of data points	Method	Reference
			750 K	800 K	850 K			
1.	−740.19 + 0.39520. T (±0.3[a])	760–853	−443.8[b]	−424.0	−404.3	13	Manometry	This work
2.	−726.77 + 0.37671. T (±1.7[a])	718–909	−444.2	−425.4	−406.6	4	Manometry	Le Chatelier [26]
3.	−733.89 + 0.38739. T (±0.3[a])	718–880	−443.4	−424.0	−404.6	16	Manometry	Reinders and Hamburger [27]
4.	−736.01 + 0.39005. T (±0.3[a])	757–912	−443.5[b]	−424.0	−404.5	19	Manometry	Otto [28]
5.	−740.42 + 0.39276. T (±0.49[a])	835–891	−445.9[b]	−426.2[b]	−406.6	4	Thermogravimetry	Abadir et al. [29]
6.	−736.78 + 0.39072. T[c]	763–873	−443.7[b]	−424.2	−404.7	–	Manometry	Kharif et al. [30]
7.	−710.04 + 0.35668. T (±0.74)	696–812	−442.5	−424.7	−406.9[b]	17	EMF method	Mallika and Sreedharan [31]

[a] Error shown is standard deviation from mean calculated from the raw data.
[b] Extrapolated value.
[c] Error not reported.

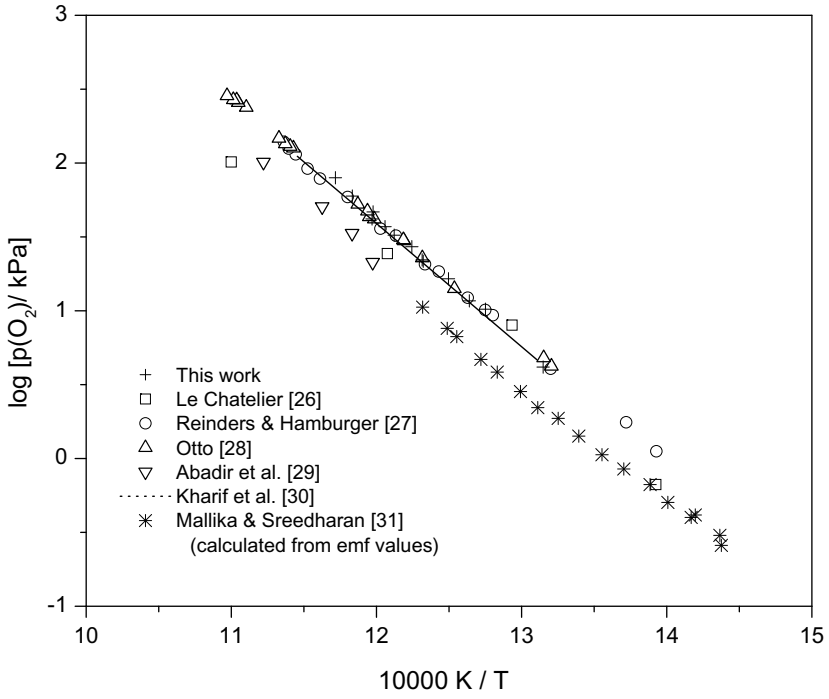

Fig. 4. Comparison of measured $\log p(O_2)$ (kPa) vs. $1/T$ (K) data for the binary mixture $\langle Pb_3O_4\rangle$–$\langle$β-PbO$\rangle$ with those data reported in literature.

Table 5
Thermochemical properties of the phase field $[PbO]_{ss}$–$\{Pb–Bi\}_{alloy}$–$\langle Pb_5Bi_8O_{17}\rangle$ derived from emf Cell-II and manometric studies

T (K)	E (mV)	a_{Pb}	x_{Pb}	x_{Bi}	a_{Bi}	$\Delta_f G^\circ_m\langle Pb_5Bi_8O_{17}\rangle$ (kJ mol^{-1})
667.9	672.1	0.0153	0.0318	0.9682	0.9680	−2322.3
679.9	666.9	0.0171	0.0350	0.9650	0.9647	−2304.4
692.7	661.1	0.0190	0.0384	0.9616	0.9613	−2284.7
704.7	654.2	0.0199	0.0398	0.9602	0.9598	−2262.8
716.9	647.6	0.0211	0.0417	0.9583	0.9579	−2241.5
729.3	642.0	0.0231	0.0453	0.9547	0.9542	−2222.5
742.1	633.3	0.0232	0.0449	0.9551	0.9546	−2195.9
753.6	627.5	0.0247	0.0474	0.9526	0.9520	−2176.9
766.4	620.9	0.0264	0.0500	0.9500	0.9494	−2155.3
778.9	615.2	0.0287	0.0538	0.9462	0.9455	−2136.1
791.6	608.3	0.0301	0.0560	0.9440	0.9432	−2113.9
802.2	602.1	0.0310	0.0571	0.9429	0.9421	−2094.3
816.3	595.2	0.0333	0.0608	0.9392	0.9382	−2071.4
828.8	589.1	0.0355	0.0642	0.9358	0.9347	−2051.3
836.4	584.9	0.0364	0.0654	0.9346	0.9335	−2037.8
836.5	584.6	0.0362	0.0650	0.9350	0.9339	−2037.0

The cell reaction can be represented as below

$$6(O_2) + 8Bi_{Pb–Bi} + 5[\beta\text{-PbO}]_{ss} \Longleftrightarrow \langle Pb_5Bi_8O_{17}\rangle. \quad (10)$$

The standard molar Gibbs energy of formation of $\langle Pb_5Bi_8O_{17}\rangle$ can be related to the measured emf values by the following expression:

$$\Delta_f G^\circ_m\langle Pb_5Bi_8O_{17}\rangle = -24FE + 8RT \ln a_{Bi} + 5\Delta_f G^\circ_m\langle\beta\text{-PbO}\rangle + 5RT \ln a_{PbO}. \quad (11)$$

Equilibrium activities of bismuth and lead oxide, namely a_{Bi} and a_{PbO} were determined as described below.

The equilibrium oxygen pressures of the following equilibrium were measured by the manometric technique by taking a mixture of $[\beta\text{-PbO}]_{ss}$, $\langle Pb_3O_4\rangle$ and $\langle Pb_5Bi_8O_{17}\rangle$ as sample:

$$3[\beta\text{-PbO}]_{ss} + 1/2(O_2) \Longleftrightarrow \langle\ Pb_3O_4\rangle. \quad (12)$$

The measured values of oxygen partial pressure as a function of temperature are given in Table 6. The data were least-squares fitted and are given by the following expression:

$$\log(p(O_2)/\text{kPa}) \pm 0.02 = 11.63–8249/T \quad (745–853\ \text{K}). \quad (13)$$

The error given is the standard deviation from the straight line. The $\Delta_r G^\circ(T)$ for the reaction (12) can be represented as

$$\Delta_r G^\circ(\text{T}) = \Delta_f G^\circ_m\langle Pb_3O_4\rangle - 3\Delta_f G^\circ_m\langle\beta\text{-PbO}\rangle - 3RT \ln a_{PbO} = (1/2)RT \ln p(O_2). \quad (14)$$

The values of $\Delta_r G^\circ(T)$ was calculated using data given by Eq. (13) and is given as

$$\Delta_r G^\circ(T) \pm 0.10\ \text{kJ} = -78.96 + 0.09213\ T(\text{K}) \quad (745–853\ \text{K}). \quad (15)$$

The error shown is the standard deviation from the straight line.

The activity of PbO in $[\beta\text{-PbO}]_{ss}$, a_{PbO}, that coexists with $\langle Pb_3O_4\rangle$ and $\langle Pb_5Bi_8O_{17}\rangle$ can be computed using the

Table 6
Measured equilibrium oxygen pressures over the $\langle Pb_3O_4\rangle$–$[PbO]_{ss}$–$\langle Pb_5Bi_8O_{17}\rangle$ phase field at different temperatures

T (K)	$p(O_2)$ (kPa)	t (h)[a]
744.5	3.40	24
754.8	5.19	23
763.3	6.91	22
773.8	9.55	22
784.5	12.61	21
792.8	17.30	20
804.5	23.68	19
813.6	30.04	17
824.3	40.94	16
833.4	53.54	14
841.5	70.51	14
842.4	70.29	13
843.9	70.47	13
853.1	91.59	12

[a] Approximate time taken for equilibrium measurement.

standard molar Gibbs energy data on $\langle Pb_3O_4\rangle$ obtained in this work and data on $\langle$β-PbO$\rangle$ reported by us earlier [21].

The deduced dependence of a_{PbO} on temperature is given by the following expression:

$$\log(a_{PbO}) \pm 0.01 = 7.333 \times 10^{-2} - 74.7\ \mathrm{K}/T \quad (745\text{–}853\ \mathrm{K}). \tag{16}$$

It is to be pointed out that the three-phase equilibria studied by manometry and emf of Cell-II, viz., $\langle Pb_3O_4\rangle$–[β-PbO]$_{ss}$–$\langle Pb_5Bi_8O_{17}\rangle$ and $\{Bi\}_{Pb\text{-}Bi}$–[β-PbO]$_{ss}$–$\langle Pb_5Bi_8O_{17}\rangle$ have the common two-phase boundary, namely [β-PbO]$_{ss}$-$\langle Pb_5Bis_8O_{17}\rangle$ and hence activity of lead oxide in [β-PbO]$_{ss}$ would be same in both the phase fields at a given temperature.

A detailed review of the thermochemical data on the Pb–Bi system has been carried out by Gokcen [33] and had recommended the activity-composition-temperature relations for Pb and Bi in Pb–Bi alloys. The emf data from Cell-II can be used to determine the activity of Pb by considering the following equilibrium at the sample electrode:

$$[Pb]_{Pb\text{–}Bi} + 1/2(O_2) \Longleftrightarrow [\beta\text{-PbO}]_{ss}. \tag{17}$$

The activity of Pb, a_{Pb} can be expressed as

$$RT \ln a_{Pb} = \Delta_f G^\circ{}_m\langle\beta\text{-PbO}\rangle + RT \ln a_{PbO} - 1/2RT \ln p(O_2). \tag{18}$$

Values of a_{Pb} were derived using the values of a_{PbO} from expression (16), $p(O_2)$ data from the measured emf values and data on $\Delta_f G^\circ{}_m\langle\beta\text{-PbO}\rangle$ [21]. Using the a_{Pb} values, a_{Bi} values were computed using the activity-composition-temperature relations for the Pb–Bi system recommended by Gokcen [33].

Using values of a_{PbO} and a_{Bi}, the standard molar Gibbs energy of formation of $\langle Pb_5Bi_8O_{17}\rangle$ was derived employing expression (11). The derived thermochemical values are shown in Table 5. Least-squares analysis of the values of the Gibbs energy of formation of $\langle Pb_5Bi_8O_{17}\rangle$ yielded the following expression:

$$\Delta_f G^\circ{}_m\langle Pb_5Bi_8O_{17}\rangle \pm 2.9\ \mathrm{kJ} = -3463.8 + 1.7056\ T(\mathrm{K}) \quad (668\text{–}837\ \mathrm{K}). \tag{19}$$

The data on $\Delta_f G^\circ{}_m\langle Pb_5\ Bi_8O_{17}\rangle$ have been determined for the first time. No experimental or estimated values of thermodynamic functions are available for this compound in the literature to compare with the present results.

3.4. Standard molar Gibbs energy of formation of $\langle PbBi_{12}O_{19}\rangle$

The equilibrium oxygen pressures of the following equilibrium were measured as a function of temperature by the manometric method:

$$\langle Pb_5Bi_8O_{17}\rangle + 13/18(O_2) \Longleftrightarrow 13/9\langle Pb_3O_4\rangle + 2/3\langle PbBi_{12}O_{19}\rangle. \tag{20}$$

The measured oxygen partial pressures at different experimental temperatures are given in Table 7. The least-squares analysis of the data yielded the following expression:

$$\log(p(O_2)/\mathrm{kPa}) \pm 0.02 = 10.50\text{–}7296/T \quad (784\text{–}849\ \mathrm{K}). \tag{21}$$

The error given is the standard deviation from the straight line.

The $\Delta_r G^\circ(T)$ for the reaction (20) can be represented as

$$\Delta_r G^\circ(\mathrm{T}) = (13/9)\Delta_f G^\circ{}_m\langle Pb_3O_4\rangle + (2/3)\Delta_f G^\circ{}_m\langle PbBi_{12}O_{19}\rangle - \Delta_f G^\circ{}_m\langle Pb_5Bi_8O_{17}\rangle = (13/18)RT \ln p(O_2). \tag{22}$$

Table 7
Measured equilibrium oxygen pressures of temperature over the $\langle Pb_3O_4\rangle$–$\langle Pb_5Bi_8O_{17}\rangle$–$\langle PbBi_{12}O_{19}\rangle$ phase field at different temperatures

T (K)	$p(O_2)$ (kPa)	t (h)[a]
784.1	15.93	35
787.4	16.89	34
790.9	19.45	33
795.0	21.03	31
799.5	24.12	29
804.3	25.81	28
808.4	29.04	27
812.0	30.81	27
816.6	36.84	26
821.1	40.50	26
825.1	45.49	25
828.9	48.84	25
833.8	55.76	24
833.9	58.04	24
836.5	57.85	23
840.4	62.50	22
842.9	71.26	22
848.5	83.86	21

[a] Approximate time taken for equilibrium measurement.

$\Delta_r G^\circ(T)$ was calculated using the measured oxygen pressure data (Eq. (21)) and is given as below

$$\Delta_r G^\circ(T) \pm 0.16\ \text{kJ} = -101.00 + 0.11756\ T(\text{K}) \quad (784\text{–}849\ \text{K}). \tag{23}$$

Using the data on $\Delta_f G^\circ_m\langle Pb_3O_4\rangle$ and $\Delta_f G^\circ_m\langle Pb_5Bi_8O_{17}\rangle$ from expressions (5) and (19), respectively, $\Delta_f G^\circ_m\langle PbBi_{12}O_{19}\rangle$ was computed and is given by

$$\Delta_f G^\circ_m\langle PbBi_{12}O_{19}\rangle \pm 4.4\ \text{kJ} = -3743.4 + 1.8784\ T(\text{K}) \quad (784\text{–}849\ \text{K}). \tag{24}$$

The data on $\Delta_f G^\circ_m\langle PbBi_{12}O_{19}\rangle$ has been determined for the first time. No experimental or estimated values of thermodynamic functions of this compound are available in the literature for comparing them with the present results.

3.5. Computations of composition of Pb–Bi alloy in other phase fields

From the measured standard molar Gibbs energy of formation of $\langle Pb_5Bi_8O_{17}\rangle$ and $\langle PbBi_{12}O_{19}\rangle$, the composition of the {Pb–Bi} alloys in the two other three-phase fields below the PbO–Bi_2O_3 pseudo-binary line can be computed. $\langle Bi_2O_3\rangle$ is also reported to form terminal solid solution with $\langle PbBi_{12}O_{19}\rangle$ [7]. As mentioned earlier, our experiments to determine the activity of $\langle Bi_2O_3\rangle$, $a_{Bi_2O_3}$, in equilibrium with $\langle Pb_3O_4\rangle$ and $\langle PbBi_{12}O_{19}\rangle$ by measuring the equilibrium oxygen pressures were not successful. Hence, in these computations $\langle Bi_2O_3\rangle$ was assumed to be a pure phase (i.e., $a_{Bi_2O_3} = 1$).

3.5.1. $\langle Pb_5Bi_8O_{17}\rangle$–$\langle PbBi_{12}O_{19}\rangle$–$\{Pb\text{–}Bi\}_y$ phase field

To determine the composition of the alloy $\{Pb\text{–}Bi\}_y$, the following equilibria were considered:

$$2\{Bi\}_{Pb\text{–}Bi} + 3/2(O2) \leftrightarrow [Bi_2O_3]_{Pb\text{–}Bi}, \tag{25}$$

$$\{Pb\}_{Pb\text{–}Bi} + 1/2(O_2) \leftrightarrow [PbO]_{Pb\text{–}Bi}. \tag{26}$$

The corresponding thermochemical expressions are given by

$$2\ RT \ln a_{Bi} + 3/2\ RT \ln p(O_2) = \Delta_f G^\circ_m\langle Bi_2O_3\rangle + RT \ln a_{Bi_2O_3}, \tag{27}$$

$$RT \ln a_{Pb} + 1/2\ RT \ln p(O_2) = \Delta_f G^\circ_m\langle \beta\text{-PbO}\rangle + RT \ln a_{PbO}. \tag{28}$$

Since $\Delta\overline{G}(O_2)$ [$= RT \ln p(O_2)$] in the equilibria (25) and (26) are equal

$$2/3\left[\Delta_f G^\circ_m\langle Bi_2O_3\rangle + RT \ln a_{Bi_2O_3} - 2\ RT \ln a_{Bi}\right] = 2[\Delta_f G^\circ_m\langle \beta - \ PbO\rangle + RT \ln a_{PbO} - RT \ln a_{Pb}].$$

This can be rearranged to give the following expression:

$$2/3\left[\Delta_f G^\circ_m\langle Bi_2O_3\rangle + RT \ln a_{Bi_2O_3}\right] - 2[\Delta_f G^\circ_m\langle \beta\text{-PbO}\rangle + RT \ln a_{PbO}] = RT \ln\left(a_{Bi}^{4/3}/a_{Pb}^2\right). \tag{29}$$

$RT \ln a_{Bi_2O_3}$ and $RT \ln a_{PbO}$ may be derived by considering the following equilibria:

$$5[PbO]_{Pb\text{–}Bi} + 4[Bi_2O_3]_{Pb\text{–}Bi} \Longleftrightarrow \langle Pb_5Bi_8O_{17}\rangle \tag{30}$$

$$[PbO]_{Pb\text{–}Bi} + 6[Bi_2O_3]_{Pb\text{–}Bi} \Longleftrightarrow \langle PbBi_{12}O_{19}\rangle. \tag{31}$$

The corresponding thermochemical expressions are given by

$$5\Delta_f G^\circ_m\langle \beta\text{-PbO}\rangle + 5RT \ln a_{PbO} + 4\Delta_f G^\circ_m\langle Bi_2O_3\rangle + 4RT \ln a_{Bi_2O_3} = \Delta_f G^\circ_m\langle Pb_5Bi_8O_{17}\rangle, \tag{32}$$

$$\Delta_f G^\circ_m\langle \beta\text{-PbO}\rangle + RT \ln a_{PbO} + 6\Delta_f G^\circ_m\langle Bi_2O_3\rangle + 6RT \ln a_{Bi_2O_3} = \Delta_f G^\circ_m\langle PbBi_{12}O_{19}\rangle. \tag{33}$$

By substituting the values for $\Delta_f G^\circ_m\langle \beta\text{-PbO}\rangle$ and $\Delta_f G^\circ_m\langle Bi_2O_3\rangle$ from recently published work [21,22] and $\Delta_f G^\circ_m\langle Pb_5Bi_8O_{17}\rangle$ and $\Delta_f G^\circ_m\langle PbBi_{12}O_{19}\rangle$ values obtained from the present work, the two unknowns, viz., $RT \ln a_{PbO}$ and $RT \ln a_{Bi_2O_3}$ corresponding to this phase field could be obtained. These values of $RT \ln a_{PbO}$ and $RT \ln a_{Bi_2O_3}$ were substituted in the expression (29) and the equilibrium activity ratio of the elements in $\{Pb\text{–}Bi\}_y$ in the three-phase field, viz., $(a_{Bi}^{4/3}/a_{Pb}^2)$ was obtained. The composition of $\{Pb\text{–}Bi\}_y$ alloy that matches this activity ratio at the chosen temperature was then deduced from the data on activity–composition–temperature relations of the Pb–Bi alloy [33]. Table 8 lists the computed compositions of the alloy in this phase field as a function of temperature.

3.5.2. $\langle PbBi_{12}O_{19}\rangle$–$\langle Bi_2O_3\rangle$–$\{Pb\text{–}Bi\}_z$ phase field

Under equilibrium, the following reactions were considered:

$$2\{Bi\}_{Pb\text{–}Bi} + 3/2(O_2) \leftrightarrow \langle Bi_2O_3\rangle \tag{34}$$

$$\{Pb\}_{Pb\text{–}Bi} + 1/2(O_2) \leftrightarrow [PbO]_{Pb\text{–}Bi} \tag{35}$$

Table 8
Equilibrium alloy compositions computed at various temperatures

T (K)	$\{Pb\text{–}Bi\}_x$	$\{Pb\text{–}Bi\}_y$	$\{Pb\text{–}Bi\}_z$
673	$Pb_{0.034}Bi_{0.966}$	$Pb_{0.029}Bi_{0.971}$	$Pb_{0.003}Bi_{0.997}$
773	$Pb_{0.052}Bi_{0.948}$	$Pb_{0.050}Bi_{0.950}$	$Pb_{0.008}Bi_{0.992}$
823	$Pb_{0.062}Bi_{0.938}$	$Pb_{0.061}Bi_{0.939}$	$Pb_{0.013}Bi_{0.987}$

$\{Pb\text{–}Bi\}_x$: equilibrium alloy composition that coexists with $\langle \Phi\text{-}Pb_5Bi_8O_{17}\rangle$–$[\beta\text{-PbO}]_{ss}$.
$\{Pb\text{–}Bi\}_y$: equilibrium alloy composition that coexists with $\langle \Phi\text{-}Pb_5Bi_8O_{17}\rangle$–$\langle PbBi_{12}O_{19}\rangle$.
$\{Pb\text{–}Bi\}_z$: equilibrium alloy composition that coexists with $\langle PbBi_{12}O_{19}\rangle$–$\langle Bi_2O_3\rangle$.

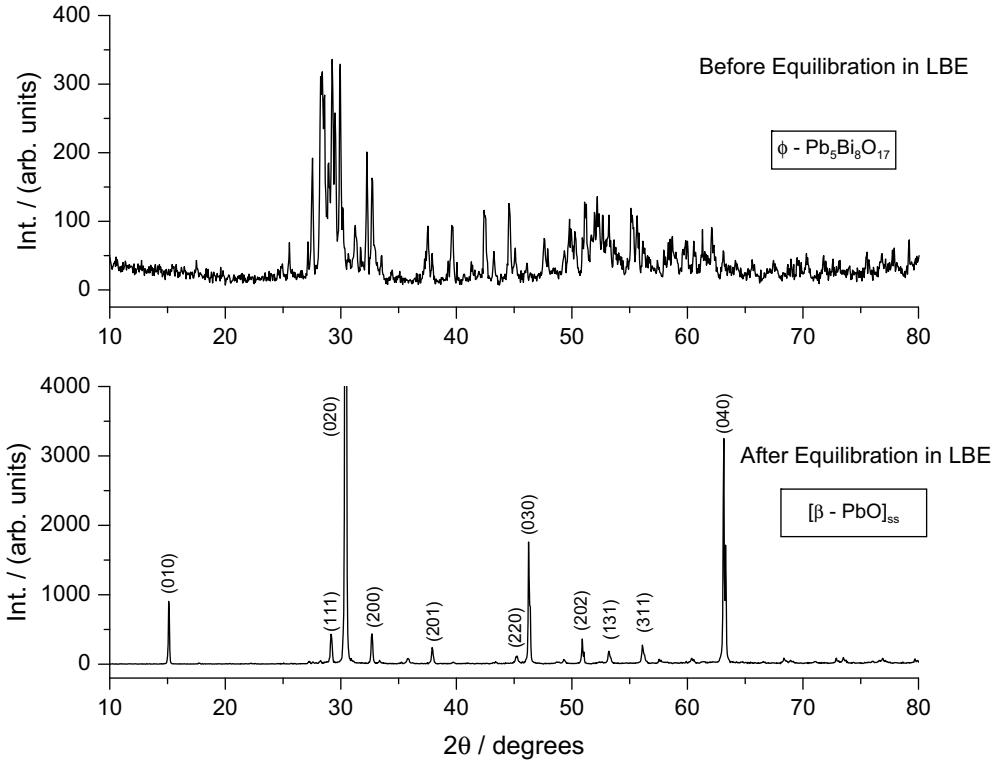

Fig. 5. X-ray diffraction patterns of $\langle \phi\text{-}Pb_5Bi_8O_{17} \rangle$ film before and after equilibration in oxygen saturated LBE at 823 K. After equilibration, the orthorhombic (yellow form) $[\beta\text{-}PbO]_{ss}$ phase coexists with LBE.

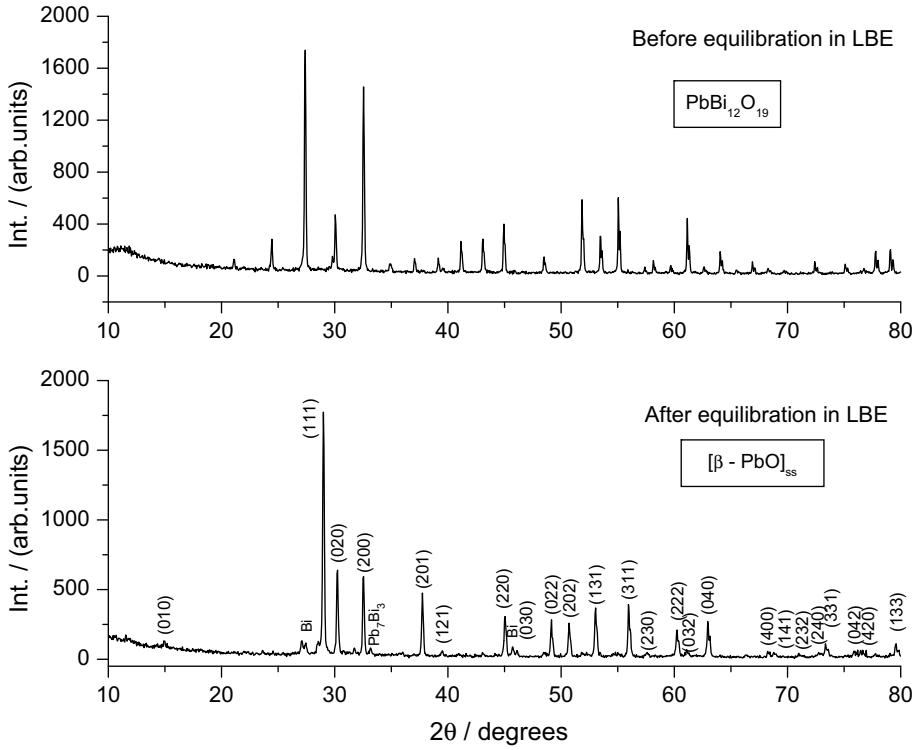

Fig. 6. X-ray diffraction patterns of $\langle PbBi_{12}O_{19} \rangle$ films before and after equilibration in oxygen saturated LBE at 823 K. After equilibration, the orthorhombic (yellow form) $[\beta\text{-}PbO]_{ss}$ phase coexists with LBE.

The corresponding thermochemical expressions are given by

$$2\ RT\ \ln a_{\mathrm{Bi}} + 3/2\ RT\ \ln p(\mathrm{O_2}) = \Delta_f G^{\circ}{}_m\langle \mathrm{Bi_2O_3}\rangle \quad (36)$$

$$RT\ \ln a_{\mathrm{Pb}} + 1/2RT\ \ln p(\mathrm{O_2}) = \Delta_f G^{\circ}{}_m\langle \beta\text{-PbO}\rangle + RT\ \ln a_{\mathrm{PbO}} \quad (37)$$

Since $\Delta\overline{G}(\mathrm{O_2})$ are equal in the above reactions (34) and (35), using the expressions (36) and (37), it can be written as

$$2/3[\Delta_f G^{\circ}{}_m\langle \mathrm{Bi_2O_3}\rangle - 2\ RT\ \ln a_{\mathrm{Bi}}] = 2[\Delta_f G^{\circ}{}_m\langle \beta - \mathrm{PbO}\rangle + RT\ \ln a_{\mathrm{PbO}} - \mathrm{RT}\ \ln a_{\mathrm{Pb}}], \quad (38)$$

$$(2/3)\Delta_f G^{\circ}{}_m\langle \mathrm{Bi_2O_3}\rangle - 2[\Delta_f G^{\circ}{}_m\langle \beta - \mathrm{PbO}\rangle + RT\ \ln a_{\mathrm{PbO}}] = RT\ \ln\left(a_{\mathrm{Bi}}^{4/3}/a_{\mathrm{Pb}}^{2}\right). \quad (39)$$

$RT\ \ln a_{\mathrm{PbO}}$ can be derived by considering the equilibrium

$$[\mathrm{PbO}]_{\mathrm{Pb-Bi}} + 6\langle \mathrm{Bi_2O_3}\rangle = \langle \mathrm{PbBi_{12}O_{19}}\rangle. \quad (40)$$

The corresponding thermochemical expression is given by

$$RT\ \ln a_{\mathrm{PbO}} = \Delta_f G^{\circ}{}_m\langle \mathrm{PbBi_{12}O_{19}}\rangle - \Delta_f G^{\circ}{}_m\langle \beta\text{-PbO}\rangle - 6\Delta_f G^{\circ}{}_m\langle \mathrm{Bi_2O_3}\rangle. \quad (41)$$

By substituting the values for $\Delta_f G^{\circ}{}_m\langle \beta\text{-PbO}\rangle$ and $\Delta_f G^{\circ}{}_m\langle \mathrm{Bi_2O_3}\rangle$ from Ref. [21,22] and $\Delta_f G^{\circ}{}_m\langle \mathrm{PbBi_{12}O_{19}}\rangle$ value obtained from the present work, $RT\ \ln a_{\mathrm{PbO}}$ corresponding to this phase field could be calculated. By substituting the value of $RT\ \ln a_{\mathrm{PbO}}$, the composition of the $\{\mathrm{Pb–Bi}\}_z$ alloy that matched the condition of the activity ratio of the metals given in expression (39) was calculated using the data on the activity–composition–temperature relation of Pb and Bi in Ref. [33]. Table 8 lists the compositions of the alloy in this phase field as a function of temperature.

3.6. Confirmatory experiments to characterize the oxide that coexists with LBE

The phase equilibrium study (Fig. 3) and computations of alloy compositions given in Section 3.5 have shown that the oxide phase that coexists with LBE is $[\beta\text{-PbO}]_{ss}$. Confirmatory evidence of this was obtained by XRD characterization of the products formed on equilibrating the films of $\langle \mathrm{Pb_5Bi_8O_{17}}\rangle$ and $\langle \mathrm{PbBi_{12}O_{19}}\rangle$ with oxygen saturated LBE. XRD patterns of the films before and after equilibration are shown in Figs. 5 and 6, respectively. As these patterns clearly reveal, the coexisting phase with LBE is orthorhombic (yellow) $[\beta\text{-PbO}]_{ss}$ phase. Small quantities of either $\langle \mathrm{Pb_7Bi_3}\rangle$ alone or $\langle \mathrm{Pb_7Bi_3}\rangle$ and $\langle \mathrm{Bi}\rangle$ are also seen which are expected to be formed when LBE is cooled to room temperature from high-temperatures.

4. Conclusions

The partial ternary phase diagram of Pb–Bi–O system has been determined by equilibration of phase mixtures and their characterization by XRD. The standard molar Gibbs energy of formation of $\langle \mathrm{Pb_5Bi_8O_{17}}\rangle$ and $\langle \mathrm{PbBi_{12}O_{19}}\rangle$ was determined by measuring equilibrium oxygen partial pressures in appropriate ternary phase fields employing a manometric technique in conjunction with the emf method using a solid oxide electrolyte-based cell. These reported thermochemical data are first of their kind. Using these thermochemical data, the compositions of the {Pb–Bi} alloy that coexist in different phase fields were computed. The computations show that the oxide that coexists with LBE is $[\beta\text{-PbO}]_{ss}$ and this has been confirmed by supplementary experiments.

Acknowledgements

The authors sincerely acknowledge Mr M.K. Elumalai for his help during experiments. The authors sincerely acknowledge Mrs Kitheri Joseph for her help in DTA analysis. The authors also gratefully acknowledge Mrs Kitheri Joseph, Mr K.H. Mahendran and Dr R. Sridharan for helpful discussions and Dr K.V.G. Kutty and his group for their help in recording XRD pattern. The authors express their sincere thanks to Dr Rajendra Prasad, former member of Fuel Chemistry Division, BARC for his technical suggestions.

References

[1] B.F. Gromov (Ed.), Proceedings of Heavy Liquid Metal Coolants in Nuclear Technology (HLMC-98), vol. 1&2, SSC RF-IPPE, Obninsk, 1999.
[2] T.B. Massalski, H. Okamoto, P.R. Subramanian, L. Kacprzak (Eds.), Binary Alloys Phase Diagrams, 2nd Ed., The Materials Information Society, USA, 1990.
[3] B.F. Gromov, G.I. Toshinsky, V.V. Checkunov, Yu.I. Orlov, Yu.S. Belomytsev, I.N. Gorelov, A.G. Karabash, M.P. Leonchuk, D.V. Pankratov, Yu.G. Pahkin, in: B.F. Gromov (Ed.), Proceedings of Heavy Liquid Metal Coolants in Nuclear Technology (HLMC-98), vol. 1, SSC RF-IPPE, Obninsk, 1999, p. 14.
[4] N. Li, J. Nucl. Mater. 300 (2002) 73.
[5] G. Müller, A. Heinzel, G. Schumacher, A. Weisenburger, J. Nucl. Mater. 321 (2003) 256.
[6] P.N. Martynov, Yu.I. Orlov, in: B.F. Gromov (Ed.), Proceedings of Heavy Liquid Metal Coolants in Nuclear Technology (HLMC-98), vol. 2, SSC RF-IPPE, Obninsk, 1999, p. 565.
[7] R.M. Biefeld, S.S. White, J. Am. Ceram. Soc. 64 (1981) 182.
[8] A.D. Murray, C.R.A. Catlow, F. Beech, J. Drennan, J. Solid State Chem. 62 (1986) 290.
[9] S. Mazumdar, Ind. J. Phys. 67A (1993) 45.
[10] N. Rangavittal, T.N. Gururow, C.N.R. Rao, Eur. J. Solid State Inorg. Chem. 31 (1994) 409.
[11] F. Honnart, J.C. Boivin, D. Thomas, K.J. De Vries, Solid State Ionics 9&10 (1983) 921.
[12] G.A. Bordovskii, A.B. Zarkoi, Phys. Status Solidi 87 (1985) K7.
[13] N.M. Sammes, R.J. Phillips, M.G. Fee, Solid State Ionics 69 (1994) 121.
[14] M.G. Fee, N.M. Sammes, G. Tompsett, T. Stoto, A.M. Cartner, Solid State Ionics 95 (1997) 183.
[15] A. Watanabe, Y. Kitami, S. Takenouchi, J.O. Bovin, N. Sammes, J. Solid State Chem. 144 (1999) 195.
[16] Y. Zhang, N. Sammes, Y. Du, Solid State Ionics 124 (1999) 179.
[17] M. Gemmi, L. Righi, G. Calestani, A. Migliori, A. Speghini, M. Santarosa, M. Bettinelli, Ultramicroscopy 84 (2000) 133.

[18] M.G. Fee, N.J. Long, Solid State Ionics 86–88 (1996) 733.
[19] M. Santarosa, L. Righi, M. Gemmi, A. Speghini, A. Migliori, G. Calestani, M. Bettinelli, J. Solid State Chem. 144 (1999) 255.
[20] L. Righi, G. Calestani, M. Gemmi, A. Migliori, M. Bettinelli, Acta Cryst. B 57 (2001) 237.
[21] Rajesh Ganesan, T. Gnanasekaran, Raman S. Srinivasa, J. Nucl. Mater. 320 (2003) 258.
[22] Rajesh Ganesan, T. Gnanasekaran, Raman S. Srinivasa, J. Chem. Thermodyn. 35 (2003) 1703.
[23] Database sets 1-49 and 70-92, PCPDFWIN Version: 2.4, JCPDS-International Centre for Diffraction Data, 2003.
[24] Rajesh Ganesan, T. Gnanasekaran, Raman S. Srinivasa, J. Nucl. Mater. 349 (2006) 133.
[25] A. Braileanu, M. Zaharescu, D. Crisan, E. Segal, J. Therm. Anal. 49 (1997) 1197.
[26] M.H. Le Chatelier, Bull. Soc. Chim. France 17 (1897) 791 (in French).
[27] W. Reinders, L. Hamburger, Z. Anorg. Allg. Chem. 89 (1914) 71.
[28] E.M. Otto, J. Electrochem. Soc. 113 (1966) 525.
[29] M.F. Abadir, A.M. Gadalla, Y.M. El-Agamawi, Trans. J. Brit. Ceram. Soc. 75 (1976) 68.
[30] Ya.L. Kharif, S.I. Sin'kovskii, I.L. Nesterova, D.A. Tyurin, V.Yu. Brezhnev, P.V. Kovtunenko, Inorg. Mater. 17 (1983) 1213.
[31] C. Mallika, O.M. Sreedharan, Mater. Lett. 22 (1995) 5.
[32] O. Knacke, O. Kubaschewski, K. Hesselmann (Eds.), Themochemical Properties of Inorganic Substances, vol. 2, Springer, Berlin, 1991.
[33] N.A. Gokcen, J. Phase Equilib. 13 (1992) 21.